frontiers | Frontiers in Energy Research

TYPE Mini Review
PUBLISHED 12 April 2023
DOI 10.3389/fenrg.2023.1167024

OPEN ACCESS

EDITED BY
Eugenio Quaranta,
University of Bari Aldo Moro, Italy

REVIEWED BY
Bing Zhang,
Shenyang University of Technology, China

*CORRESPONDENCE
Ashish Alex Sam,
ashishalex.sam@vit.ac.in

SPECIALTY SECTION
This article was submitted to Carbon Capture, Utilization and Storage, a section of the journal Frontiers in Energy Research

RECEIVED 15 February 2023
ACCEPTED 28 March 2023
PUBLISHED 12 April 2023

CITATION
Sreenath S and Sam AA (2023), Hybrid membrane-cryogenic CO_2 capture technologies: A mini-review. *Front. Energy Res.* 11:1167024. doi: 10.3389/fenrg.2023.1167024

Hybrid membrane-cryogenic CO_2 capture technologies: A mini-review

S. Sreenath[1] and Ashish Alex Sam[2]*

[1]School of Mechanical Engineering, Vellore Institute of Technology, Vellore, Tamil Nadu, India, [2]CO2 Research Centre and Green Technologies, School of Mechanical Engineering, Vellore Institute of Technology, Vellore, Tamil Nadu, India

The use of membranes to capture CO_2 is a proven carbon capture technique. Gas separation membranes enhance the mole fraction of CO_2 in the feed gas. The membrane separation technique is low-cost because of its compact size, excellent energy efficiency, minimum environmental effect, simplicity of scale-up, fewer moving parts, moderate energy consumption, and ease of handling. Hybrid membrane cryogenic (HMC) and low-temperature membrane cryogenic (LTMC) are hybrid capture systems that combine the advantages of membrane and cryogenic techniques. In the HMC process, the flue gas is first pre-treated by the membrane process for CO_2 enrichment and the cryogenic process to capture the CO_2. In the LTMC process, low-temperature membrane units increase flue gas CO_2 concentration to 50%–75%, and a cryogenic process liquefies the rich CO_2 stream. Permeability and selectivity are the crucial parameters of the membrane which determine the CO_2 purity and recovery of capture. Most polymeric membranes have a trade-off of CO_2/N_2 selectivity ($\alpha_{CO2/N2}$) and CO_2 permeability (P_{CO2}). The operating temperatures also impact membrane performance. An anti-trade-off effect was observed upon cooling down by increasing P_{CO2} and $\alpha_{CO2/N2}$. With increased P_{CO2} and $\alpha_{CO2/N2}$, sub-ambient temperature-based membrane cryogenic CO_2 capture techniques will lower power consumption and energy cost for CO_2 capture (CC). This review analyses the costs and energy requirements of various HMC and LTMC configurations for CO_2 capture. The study also examines the features of the different membranes used and the effect of operating and membrane parameters on the process performance.

KEYWORDS

carbon capture, hybrid membrane cryogenic process, low temperature membrane cryogenic process, energy consumption, CO_2 capture ratio, CO_2/N_2 selectivity

1 Introduction

Fossil fuel energy systems account for 80% of the global energy demand and contribute approximately 3/4th of the global CO_2 emissions (Sharma et al., 2021). Over the last 3 decades, global CO_2 emissions rose from 20.5 Gigatonnes (Gt) in 1990 to 36.6 Gt in 2021. Although it fell by 5.8% in 2020, energy-related CO_2 emissions increased by 4.8% in 2021 (IEA, 2021; 2022). Considering the impact of CO_2 emissions on global warming and the ecological balance, developing efficient CO_2 mitigation strategies for fossil fuel power plants is called for.

CO_2 capture (CC) strategies are classified into oxy-fuel combustion, pre-combustion, and post-combustion capture (Guan, 2017). Generally, post-combustion capture

technologies are preferred for power plants, as they can be easily retrofitted into any existing power plant (Wang et al., 2017). However, they must exhibit better capture efficiency for flue gases with low CO_2 concentrations (C_o).

Absorption, adsorption, cryogenic, membrane, chemical looping cycle, and hydrate are commonly used post-combustion capture methods. Amine-based absorption separation techniques are the most mature technology but are highly corrosive, energy-intensive, and have a negative environmental impact due to solvent emission (Song, Liu, Ji, Deng, Zhao, Li, Song, et al., 2018). Membrane-based CC technologies are energy-efficient and eco-friendly but require a large surface area and depend heavily on the process operating conditions (Merkel et al., 2010). Membranes are also susceptible to fouling due to the pollutants in the flue gas (Song, Liu, Ji, Deng, Zhao, Li, Song, et al., 2018).

Cryogenic methods use distinct condensation and de-sublimation capabilities to isolate CO_2 from flue gases. Compared to competing separation approaches, the cryogenic CC technique delivers very high CO_2 capture ratio (CCR) (99.99%) and purity (99.99%) rates (Song et al., 2019). As the CO_2 is captured in the solid or liquid state, cryogenic capture methods guarantee added advantage in storing and transporting the captured CO_2. Nevertheless, cryogenic capture techniques would be expensive and energy intensive, as the C_o in most of the power plant flue gas would be very low (Baxter et al., 2009).

To overcome these challenges associated with conventional CC technologies, researchers, in recent years, have shifted their focus to hybrid capture systems, which combine the merits of two or more traditional CC techniques. Hybrid membrane cryogenic (HMC) and low-temperature membrane cryogenic (LTMC) are two such strategies that combine the advantages of membrane and cryogenic techniques. Membrane-based hybrid processes are advantageous because of their compact size, excellent energy efficiency, low environmental impact, simplicity of scale-up, fewer moving parts, moderate energy consumption, and handling. This paper evaluates the different HMC and LTMC configurations based on energy consumption and cost for CO_2 capture. The study also analyses the characteristics of the various membranes employed and the effect of operating conditions on the membrane performance.

2 Membrane gas separation

In non-reactive membranes, gas permeation occurs through the solution diffusion mechanism. The principle behind it is that gas molecules are migrated across the membranes by sorption on the feed side, followed by diffusion, and then desorption on the permeate side of the membrane. The driving force may be the concentration, pressure, or temperature differential across the feed and permeate sides of the membrane. This process' separation performance is determined by Fick's law (Fick, 1855).

$$J_i = \frac{P_i}{l}\Delta p \tag{1}$$

Where J_i signifies the gas flow, P_i the permeability, Δp the partial pressure differential across the membrane, and l the membrane thickness. The permeability of a particular gas on a membrane is given by

$$P_i = D_i \times S_i \tag{2}$$

Where D_i is the diffusion coefficient (kinetic factor), and S_i is the solubility coefficient (thermodynamic factor) (Rafiq et al., 2016). Differences in solubilities and diffusivities of the gas mixture cause gas separation.

The ideal selectivity of component A over component B is given by

$$\propto_{A/B} = \frac{P_A}{P_B} = \left(\frac{D_A S_A}{D_B S_B}\right) \tag{3}$$

Diffusion selectivity (D_A/D_B) is calculated by comparing the average intersegmental distance of polymeric chains, their individual segments' mobility, and the penetrant gases' shapes and sizes (Stannett et al., 1979). In contrast, the solubility selectivity (S_A/S_B) is affected by the free volume in the membrane matrix, the interaction between the polymer and the penetrants, and the condensability of the penetrant gases (Robeson et al., 2014).

3 Hybrid membrane cryogenic process (HMC)

The hybrid membrane cryogenic capture process combines the conventional membrane and cryogenic processes. The membrane process is used to pre-treat the flue gas for CO_2 enrichment, and the cryogenic process is used to capture the CO_2. Figure 1A shows the schematic of the HMC process. The C_o in the initial feed gas, around 2%–20%, is first raised to 50%–75% by membrane units, and this enriched CO_2 stream is then subjected to a cryogenic CC process. Increasing Co will make the process energy-efficient and cost-effective. Several HMC configurations have been reported in the literature. Proper placement of the components, selection of suitable membranes, use of multi-stage membranes, and compression and vacuum techniques to generate the required pressure difference have significantly impacted the HMC performance. The following sections discuss the critical HMC configurations and the primary operating and membrane parameters that affect its energy consumption for capture (ECC).

3.1 HMC configurations

Researchers have adapted various modifications to increase the performance and decrease the ECC of HMC processes. Some examples are multi-staging, energy-recovery systems (ERS), selective-recirculation, sweep-gas technology, *etc.* A comparison of various HMC configurations and their ECC is shown in Table 1.

Belaissaoui et al. modified the HMC process by using an Energy Recovery System (ERS). The energy recovered from the retentate was used for feed compression (Belaissaoui et al., 2012). Compared to standard MEA absorption ($4.409GJ_{th}/t_{CO2}$), the developed HMC process (C_o = 15%; $\alpha_{CO2/N2}$ = 100; CO_2 permeance P_{CO2} = 1000GPU; pressure ratio PR = 11.11) utilizes less than $3.25GJ_{th}/t_{CO2}$, with a CCR over 85% and CO_2 purity above 89%.

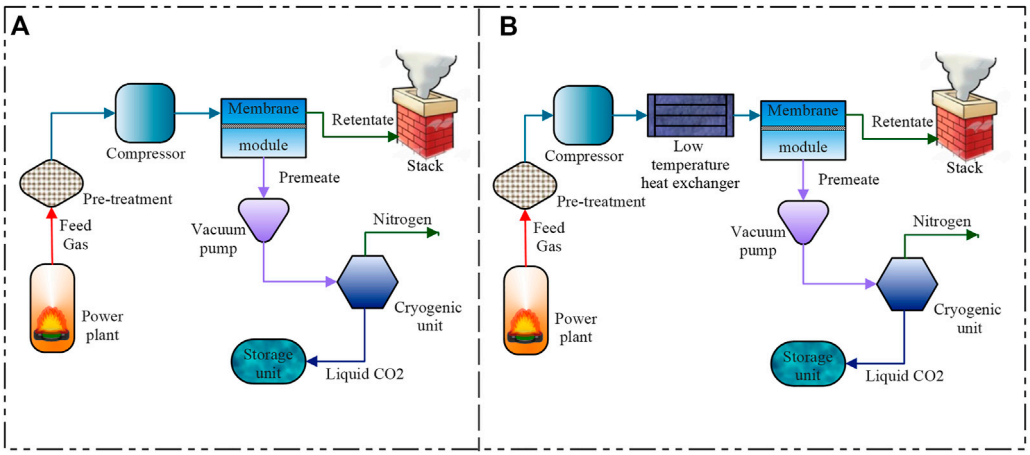

FIGURE 1
Schematic representation of **(A)** hybrid membrane cryogenic (HMC) process, **(B)** low-temperature membrane cryogenic (LTMC) process.

TABLE 1 HMC process CO_2 capture target and energy penalty comparisons.

Sl no.	Configuration	CO_2/N_2 selectivity	Membrane operating pressure		CO_2 capture targets		Specific energy consumption (GJ/ton$_{CO2}$)	References
			Feed (bar)	Permeate (bar)	Recovery (%)	Purity (%)		
1	HMC process with Air sweep	50	2	0.2	90	95		Merkel *et al.* (2010)
2	HMC with ERS	50 to 100	1	0.0086 to 0.0090	95	99.9	2.7 to 3.16	Belaissaoui *et al.* (2012)
3	Multi-stage membrane with CO_2 recirculation and oxygen enrichment	50	1.16	0.22	90	95	1	Scholes *et al.* (2013)
4	Single stage HMC	200	2	0.2	>90	>95	1.11	Zhang *et al.* (2014)
5	Multi-stage HMC with permeate recirculation	50	10	20	97.9	94.2	1.25	Shafiee *et al.* (2017)
6	HMC with SEGR	50	2	0.2	>80	99.5	1.2456	Baker *et al.* (2017)
7	Multi-stage HMC with air sweep	55 to 65	2 to 4	0.2 to 0.5	90	95	0.94 to 1.08	Mat and Lipscomb (2019)
8	HMC with N_2 selective membrane	50(N_2/CO_2)	3.6	0.6	86	94.9	1.46	Li, Lian, Zhang, Deng, *et al.* (2022)

Scholes et al. redesigned the three-stage HMC configuration proposed by (Merkel et al., 2010). The modified configuration included a two-stage membrane with CO_2 recirculation and oxygen enrichment (Scholes et al., 2013). The permeate from stage 1 (enriched CO_2) was passed on to the cryogenic capture process, whereas the retentate moved to the stage 2 membrane, where the permeate was recirculated using the sweep gas. A separate membrane configuration was included to enrich oxygen in the sweep gas. It was observed that compared to Merkel et al. Configuration (0.93 GJ/t$_{CO2}$), the modified HMC process (C_o = 13%; $\alpha_{CO2/N2}$ = 50; P_{CO2} = 1000GPU; PR = 10) reduced capital costs with a slight increase in ECC (1 GJ/t$_{CO2}$).

Shafiee et al. optimised the performance of a three-stage HMC process with permeate recirculation using Genetic Algorithm (Shafiee et al., 2017). For the optimised configuration (C_o = 14%; $\alpha_{CO2/N2}$ = 50; P_{CO2} = 152 GPU), the ECC was 1.377 GJ/t$_{CO2}$ with a CO_2 purity of 94.1% and 97.9% CCR.

Baker et al. modified the HMC process using exhaust gas recycling (S-EGR). By pre-concentrating CO_2 through S-EGR, a significant reduction in the ECC for CO_2 capture was observed (Baker et al., 2017). For a combined turbine-membrane (C_o = 13.1%; $\alpha_{CO2/N2}$ = 50; P_{CO2} = 2500GPU; PR = 5.5) capture unit with SEGR in a natural gas power plant, the cost of CO_2 capture was found to be 44$/t with an ECC of 1.2456 GJ/t$_{CO2}$.

TABLE 2 LTMC process CO_2 capture target and energy penalty comparisons.

Sl No	Flue gas/CO_2 concentration, References	CO_2/N_2 selectivity	Permeance P_{CO2} (GPU)/ [Permeability] (Barrer)	Membrane operating condition			Condensation condition		CO_2 capture targets		Specific energy consumption (GJ/ ton_{CO2})
				Feed (bar)	Permeate (bar)	Temperature (°C)	Pressure (bar)	Temperature (°C)	Recovery (%)	Purity (%)	
1	LTMC (18% CO_2), (Hasse et al., 2013)	103	[8]	16	1–2	−30	>60	−20	90		0.959
2	Coal-fired power plant (13.5% CO_2) (Song et al., 2017)	80	143	4	1	−20	1	−120	98	99.8	1.7
3	Coal-fired power plant (13.6% CO_2) (Lee, Yun, and Kim, 2019)	100	1000	2.58	0.2	−35	1	−45	90	99.9	
4	LNG power plant (4%–10% CO_2) (Lee and Kim, 2020)	100	2500	2.3	0.2	−35	30	−50		99.9	
5	Coal-fired power plant (13.6% CO_2) (Li, Lian, Zhang, Song, et al., 2022)	100	1000	2	0.2	−30	30	−45	90	96.29	1.87
6	Blast furnace (23.2% CO_2) (Li, Lian, Zhang, Song, et al., 2022)	200	1000	2	0.2	−30	30	−45	90	97.05	1.55

10.3389/fenrg.2023.1167024

TABLE 3 Temperature dependant performance of membrane materials.

Sl. No.	Membrane material	Pressure (bar)	Temperature (°C)	Permeance P_{CO2} (GPU)/ [Permeability] (Barrer)	CO_2/N_2 selectivity $\alpha_{CO2/N2}$	References
1	Dense skinned Matrimids	6.89	35	24	28	Liu *et al.* (2013)
			−20	16.6	52.5	
2	Nodular-skinned Matrimids	6.89	35	102	35	
			−20	63.3	90.5	
3	Air Liquide (AL) polyimide	~	30	[10]	20	Hasse *et al.* (2013)
			−30	[8]	103	
4	PDMS-treated Matrimids 5218	6.89	35	292	26.9	Liu *et al.* (2014)
			−40	117	135	
			−50	187	157	
5	6FDA/BPDA-DAM pyrolysed CMS	13.78	35	160	24	Joglekar *et al.* (2019)
			−20	108	109	
6	6FDA/BPDA-DAM pyrolyzed CMS1	6.89	35	2800 ± 60	30 ± 0.75	Kumar *et al.* (2019)
			−20	2440 ± 115	95 ± 4	
7	6FDA/BPDA-DAM pyrolyzed CMS2	6.89	35	3522 ± 324	26 ± 2.5	
			−20	2987 ± 373	43 ± 7.5	
8	Pebax/MIL-101	2	40	[98.2]	45.5	Song *et al.* (2020)
			−20	[28.2]	89.4	
9	Pebax/NH2-MIL- 101	2	40	[98]	23	
			−20	[30.2]	95.6	
10	PIM-1	2	30	3798	21.1	Ji, Li, Min, *et al.* (2021)
			0	2678	35.7	
			−30	1380	81.2	
11	PIM-PI-1	2	30	[1966]	17.9	Ji, Li, Shi, *et al.* (2021)
			−30	[743]	57.2	
12	PIM-DB-PI	2	30	[764]	23.2	
			−30	[457]	57.2	
13	HSBI-3-CF3	2	35	[292]	20.3	Weng *et al.* (2022)
			−20	[453]	44	
14	HSBI-4-CF3	2	35	[686]	17.5	
			−20	[903]	35.1	

Mat et al. studied an HMC process by varying the cryogenic condensation parameters (Mat and Lipscomb, 2019). It was found that for $\alpha_{CO2/N2}$ = 50, PR = 10, and condensation parameters of 15 bar and −50 °C, the specific ECC was 1.036 GJ/t_{CO2} for purity of 95% and 90% CCR.

Li et al. analysed an HMC process with multi-staging and using an N_2 selective membrane (Li, Lian, Zhang, Deng, et al., 2022). For C_o = 16.1%; $\alpha_{N2/CO2}$ = 50; P_{N2} = 1850GPU; PR = 6; the specific ECC was 1.46GJ/t_{CO2}, and the capture cost was 28.38$/$t_{CO2}$ for a purity of 94.6% and 86% CCR.

3.1.1 Effect of operating and membrane parameters

The amount of energy required for the HMC process depends on the CO_2 percentage in feed gas and operating parameters of the membrane, such as pressure and pressure ratio, and membrane parameters like selectivity and permeance.

3.1.2 Feed

The flue gas is substantial in volume, and the concentration of CO_2 in flue gas depends on the process plant. C_o in flue gas for an

LNG power plant is 2%–8%, coal-fired power plant 10%–15%, and blast furnace 20%–27% (Xu and Lin, 2017). Before being fed to the membrane, the flue gas must be pre-treated to remove the pollutants and dehydrated to remove any water content.

The feed C_o is strongly related to the purity obtained, recovery rate, and ECC. Belaissaoui et al. studied the effect of feed concentration on the purity and ECC of an HMC process employing a membrane of $\alpha_{CO2/N2}$ = 50 and 90% CCR (Belaissaoui et al., 2012). As the C_o varied from 5% to 70%, it was observed that the CO_2 purity increased from 40% to 100%, and the ECC decreased significantly. For a C_o of 30% and 50%, the corresponding ECC was 2.204 GJ/t_{CO2} and 0.331–0.551 GJ/t_{CO2}, respectively.

In another study, Belaissaoui et al. analysed feed concentration's effect on the HMC process's ECC using three distinct compression techniques (Belaissaoui et al., 2012). The impact of three different feed C_o (5, 15, and 30%) and $\alpha_{CO2/N2}$ (50 and 100) was studied. It was observed that for 15% C_o and $\alpha_{CO2/N2}$ = 100, the feed compression strategy and vacuum pumping strategy ECC was 3.25 and 2.97 GJ/t_{CO2}, and for 30% C_o, the corresponding ECC was found to be 2.07 and 2.02 GJ/t_{CO2}respectively.

A simulation was carried out by Zhang et al. for an HMC process using Aspen Plus software to study the ECC (Zhang et al., 2014). It was found that for a 13.73% C_o in feed and with a membrane $\alpha_{CO2/N2}$ = 200, the specific and total ECC are 1.22GJ_{th}/$t_{CO2}$and 161.5MJe/s.

Song et al. studied the effect of CO_2 feed concentration on energy requirement at a constant feed pressure of 3 bar. Results showed that as the concentration increased from 5% to 40%, the ECC decreased from 4.409 to 1.102 GJ/t_{CO2}, and CCR rose from 97.8% to 98.6%, with a purity of 99.9% (Song et al., 2017).

3.1.3 Pressure and pressure ratio

Pressure and pressure ratio have a significant role in membrane separation. The driving force of the membrane separation module is the pressure difference on either side of the membrane. The pressure ratio is the ratio of feed pressure to permeate pressure. Compression of feed gas or vacuum on the permeate side or both can simultaneously produce pressure difference (Merkel et al., 2010). The cost of energy to create this pressure differential is an influential factor. In power plants with an HMC capture process, the power for compression or vacuum equipment (the parasite load) consumes the central portion of the power generated (Song, Liu, Ji, Deng, Zhao, Li and Song, 2018).

Merkel et al. analysed the effect of pressure and pressure ratio in a membrane process (C_o = 11.6%; $\alpha_{CO2/N2}$ = 50; P_{CO2} = 1000GPU) by maintaining feed pressure at 2 bar and by varying permeate vacuum levels (Merkel et al., 2010). For PR = 10, a permeate purity of 45% CO_2 at a CCR of 90% was obtained. The corresponding area required was found to be 2.1 million m^2. For a pressure ratio of 4, the purity was 25% CO_2 at a CCR of 90%, and the corresponding area required was 5 million m^2. The purity was found to increase with an increase in pressure ratio, and the membrane area needed to be decreased.

Belaissaoui et al. compared the overall performance of an HMC process using three distinct compression techniques: feed compression, vacuum pumping, and feed compression with an Energy Recovery System (ERS) (Belaissaoui et al., 2012). For the vacuum pumping strategy (C_o = 15%; $\alpha_{CO2/N2}$ = 50; P_{CO2} = 1000GPU) at a permeate pressure of 8.6 mbar, the ECC was 3.29 GJ/t_{CO2} with a 52% purity. However, for feed compression with ERS, for a feed pressure of 10.41 bar and permeate pressure at 1 bar, the ECC was 3.48 GJ/t_{CO2}. In the above two cases, the specific membrane surface area required was 33.88 and 3.63m^2/t_{CO2}, respectively.

Swisher and Bhown studied the effect of feed pressure on the power needed and costing of an HMC process in pulverised coal combustion and natural gas combined cycle power plants. For a given $\alpha_{CO2/N2}$, the power requirement increased with feed pressure (1.5, 2, 3 bar). A lesser membrane area was required at higher pressures, resulting in smaller membrane costs (Swisher and Bhown, 2014).

3.1.4 CO_2/N_2 selectivity and CO_2 permeance

The efficiency with which a membrane captures CO_2 is highly dependent on the characteristics of the membrane material and the method by which CO_2 is permeated through the membrane. Key factors such as membrane selectivity (α) and permeability (P) are used to assess the membrane performance. For a given membrane, permeability is the diffusion rate of the permeate molecule, and selectivity is the ratio of the permeability of the gas pair.

Anantharaman et al. simulated an HMC process with $\alpha_{CO2/N2}$ = 80 and P_{CO2} = 1850GPU (Anantharaman et al., 2014). The cost of CC with 85% CCR was 9% lower than a conventional MEA-based CC technique.

Using a feed condition of 600 kg/s C_o = 15%; P_{CO2} = 1000GPU; 3bar of feed pressure, and a membrane area of 90 m^2, a simulation was run to examine the influence of $\alpha_{CO2/N2}$ on CCR and purity using the HMC process (Song et al., 2017). CCR increased from 81.5% to 94.5%, and purity remained at 99.9% when $\alpha_{CO2/N2}$ varied from 10 to 100. With an $\alpha_{CO2/N2}$ = 50, the hybrid process has a 2 GJ/t_{CO2} ECC. In most cases, improvements in membrane selectivity are rendered ineffective by pressure ratio limitations, whereas increases in membrane permeance reduce the system's capital cost and footprint.

4 Low-temperature membrane cryogenic hybrid process

A cohesively integrated low-temperature membrane cryogenic hybrid CO_2 recovery method consists of low-temperature units and membrane and cryogenic components. The pre-treated flue gas is first introduced to the low-temperature unit, which cools down before being sent to the membrane module to assist the gas permeation. The CO_2 selective membrane allows the CO_2 to pass through, and rich-N_2 gas is collected at the retentate side. The cryogenic unit receives an enriched-CO_2 permeate stream which is re-compressed, chilled in a heat exchanger, and phase separated in the cryo-phase separator. The separator pumps sequestration-ready liquid CO_2 or solid form (dry ice) to the storage and transportation systems. Figure 1B represents the schematics of LTMC. The operating condition and ECC for various LTMC processes are summarized in Table 2.

4.1 Effect of temperature on operating and membrane parameters

4.1.1 CO_2/N_2 selectivity and CO_2 permeance

Most gas-permeable membrane works on solution diffusion mechanisms. Membrane parameters like permeability and selectivity are greatly affected by the operating temperature. Permeability and diffusion coefficients are related to the temperature following the Arrhenius relationship, as given in Eq. 4. (Liu et al., 2013).

$$\text{Permeability } \boldsymbol{P} = \boldsymbol{P_0 e}^{\left(\frac{-E_p}{RT}\right)} \quad (4)$$

$$\text{Diffusivity } \boldsymbol{D} = \boldsymbol{D_0 e}^{\left(\frac{-E_d}{RT}\right)} \quad (5)$$

The Van't Hoff equation may characterise the relationship between temperature and the sorption coefficient.

$$\text{Sorption coefficient } \boldsymbol{S} = \boldsymbol{S_0 e}^{\left(\frac{-H_s}{RT}\right)} \quad (6)$$

where E_p is the permeation's apparent activation energy $E_p = E_d + H_s$. E_d represents the activation energy for diffusion, which represents the energy needed for a gas molecule to jump between sorption sites within the polymer matrix. H_S is the heat of sorption, primarily controlled by the condensability of the penetrant. P_0, D_0, and S_0 are the pre-exponential factors.

At sub-ambient temperatures, the gas molecule motion slows down and boosts the enthalpic effect, which enhances gas sorption coefficients. The gas diffusion selectivity across the membranes is more affected by the microporosity (fractional free volume). The reduction in fractional free volume at lower temperatures decreases diffusivity. The decrease in permeability caused by lower temperatures was mainly driven by a drop in the diffusivity, which was more significant than the effect of an increase in the solubility coefficient (Ji, Li, Min, et al., 2021; Ji, Li, Shi, et al., 2021). For a decrease in temperature, the permeability of CO_2 was less reduced than N_2 because of its compressibility and smaller particle size. Eventually brings a significant improvement in CO_2/N_2 selectivity. Increased swelling degree of the membrane at higher temperatures causes a flexible molecular chain movement and a more significant free volume fraction in molecular structure. Which raises the permeability of the non-polar gas N_2 and decreases membrane selectivity (Song et al., 2020).

The temperature dependant performance of different membrane materials is provided in Table 3. Data shows that as the temperature decreases from ambient to sub-ambient, $\alpha_{CO2/N2}$ increases, and P_{CO2} decreases up to −40 °C. Between −40 °C and −50 °C, P_{CO2} was found to increase with a decrease in temperature (Hasse et al., 2013; Liu et al., 2014). This tendency runs counter to the prediction made by the Arrhenius relationship. At low temperatures, the performance of membrane material with serial no. 10, 11, 13 & 14 on Table 3 surpass the 2019 upper bound line. Serial no. 12 surpasses the 2015 upper bound line.

4.1.2 Effect of pressure at sub-ambient temperature

Membrane performance below ambient temperature is significantly influenced by pressure. Experiments by Liu et al. on PDMS-post-treated Matrimid membrane demonstrate that the P_{CO2} rises with a rise in feed pressure and only slight variations for $\alpha_{CO2/N2}$ at sub-ambient temperatures (Liu et al., 2014). At a temperature of −50 °C and feed pressure of 10.3 bar, the $\alpha_{CO2/N2}$ and P_{CO2} were 209 and 227 GPU, respectively, with the highest P_{CO2} of 510 GPU obtained at a pressure of 24 bar.

Song et al. simulated an LTMC process and studied the effect of pressure at sub-ambient temperatures. This LTMC process can purify CO_2 to over 99% even at low pressures and obtain a maximum CCR of 98% at 4 bar feed pressure (Song et al., 2017). From 2 bar to 3 bar, an increase in pressure reduced ECC; beyond 3 bar, ECC rose steadily with flue gas pressure. High compression pressure improves CCR and purity. Over-compression leads to an increase in N_2 concentration in the permeate flow and results in reducing CCR. The literature lacks studies on the effect of pressure at low temperatures on membrane performance.

4.2 Energy and cost consideration

Air Liquide introduced a revolutionary combined sub-ambient membrane and cryogenic CO_2 recovery technology that uses high membrane permeance to absorb CO_2 from coal-fired power plant flue gas (18% C_o) with an ECC of 0.959 GJ/t_{CO2} (Hasse et al., 2013).

Song et al. proposed an LMTC process for an LNG power plant with 15% C_o. This hybrid process's ECC (1.7 GJ/t_{CO2}) was lesser than the traditional three-stage membrane capture processes (Song et al., 2017). The main reasons for this reduction in ECC were the use of LNG cold energy and the improvement in the membrane performance at sub-ambient temperatures.

Lee et al. studied a modified form of an LTMC consisting of a single membrane module with sweeping and a purification column. It could produce 99.9% purity and 90% CCR (Lee et al., 2019). Compared to a multi-stage membrane process operating at room temperature, the improved sub-ambient temperature membrane technology reduced the cost of CC by 13% and the parasitic load by 16%.

Lee and Kim analysed the LTMC process for an LNG power plant with EGR or S-EGR to concentrate the CO_2 by 4%–10% (Lee and Kim, 2020). The LNG cold was utilised for heat recovery and providing a cold environment. It was observed that the integrated process (C_o = 4%; P_{CO2} = 2500GPU; $\alpha_{CO2/N2}$ = 100) had a capture cost of \$57/t_{CO2} and, compared to a base configuration with an external refrigeration system, was able to reduce the parasite load by 70.1%.

LTMC process developed for coal-fired and blast furnace flue gas by Li. et al. uses high-selectivity membranes operating at sub-ambient temperatures conserved vacuum energy (Li, Lian, Zhang,

Song, et al., 2022). For coal-fired flue gas, (P_{CO2} = 1000GPU; $\alpha_{CO2/N2}$ = 200) instances cost 36.14\$/t_{CO2} and used 1.87 GJ/t_{CO2} ECC, compared with the base case (P_{CO2} = 1000GPU; $\alpha_{CO2/N2}$ = 50) the parasite load dropped 7.11% from 168 MW. The optimized blast furnace flue gas (P_{CO2} = 1000GPU; $\alpha_{CO2/N2}$ = 200) capture cost and ECC were 28.81 \$/t_{CO2} and 1.55 GJ/t_{CO2}. Compared with the base case, its parasite load dropped 15.55% from 17.81 MW.

5 Conclusion

Based on the above analysed information, it is evident that when compared to conventional capture technologies, HMC and LTMC technologies achieved increased CO_2 capture percentage and reduced energy consumption. This was achieved through the proper selection of membranes and optimisation of the operating conditions. Despite the growing interest in CO_2 capture using HMC and LTMC process, and the promising findings that have been reported, most of the current research was conducted in a simulated or lab context. More field testing of these strategies should be done for better understanding.

The use of a vacuum pump on permeate side was found to have reduced ECC. For an HMC process, compared to feed compression with ERS, incorporating a vacuum pump reduces ECC by 5.45%.

However, the literature lacks studies on the influence of pressure and pressure ratio on the performance of membranes at low temperatures. As the increase in pressure ratio effects the purity and required membrane area, the impact of pressure ratio in the membrane at sub-ambient temperature has to be further explored.

Similarly, high selectivity membranes reduce ECC. Membranes with high permeance reduce the required membrane area, thereby reducing the capture costs. CO_2 permeance of 10^5 GPU can be achieved in membranes by optimising porosity, pore size, and molecular structure (He et al., 2019). This paves the way for a future generation of superior membranes for various vital separations. As the performance of LTMC process depends on selectivity and permeability the characteristics of these newly developed membranes at low temperature also need to be examined.

LTMC process generally requires external refrigeration in the membrane process. For the same operating condition, compared to the HMC process, the LTMC process reduced ECC by 43.3%, mainly due to the improved performance of the membrane at low temperatures. A further reduction in ECC is possible in LNG power plants by utilising LNG cold energy. To reduce the ECC and increase CO_2 purity and recovery, further optimisation of the LTMC process is necessary. By using LNG cold energy, the temperature on the membrane side can be further reduced to −70 °C or lower. As the temperature decreased from ambient to sub-ambient (−40 °C), $\alpha_{CO2/N2}$ increased, and P_{CO2} decreased. Between −40 °C and −50 °C, P_{CO2} increased with a decrease in temperature, violating the Arrhenius relation. Literature has not caught up with the study of violations yet, and the authors strongly feel that there must be further investigation on membrane characteristics and performance at temperatures below −40°C.

Author contributions

SS: data curation and writing—original draft preparation, editing. AS: supervision, English language modification, writing—reviewing and editing.

Acknowledgments

The authors would like to thank Vellore Institute of Technology for supporting this work.

Conflict of interest

The authors declare that the research was conducted in the absence of any commercial or financial relationships that could be construed as a potential conflict of interest.

Publisher's note

References

Anantharaman, R., Berstad, D., and Roussanaly, S. (2014) 'Techno-economic performance of a hybrid membrane - liquefaction process for post-combustion CO2 capture', *Energy Procedia*, 61(1876), 1244–1247. doi:10.1016/j.egypro.2014.11.1068

Baker, R. W., Freeman, B., Kniep, J., Wei, X., and Merkel, T. (2017). CO2 capture from natural gas power plants using selective exhaust gas recycle membrane designs. *Int. J. Greenh. Gas Control* 66, 35–47. doi:10.1016/j.ijggc.2017.08.016

Baxter, L., Baxter, A., and Stephanie, B. (2009). "Cryogenic CO2 capture as a cost-effective CO2 capture process," in *26th annual international pittsburgh coal conference 2009*, 762–775. Available at: https://www.researchgate.net/publication/264875049.

Belaissaoui, B., Le Moullec, Y., Willson, D., and Favre, E. (2012). Hybrid membrane cryogenic process for post-combustion CO 2 capture. *J. Membr. Sci.* 415 (416), 424–434. doi:10.1016/j.memsci.2012.05.029

Belaissaoui, B., Willson, D., and Favre, E. (2012). Membrane gas separations and post-combustion carbon dioxide capture: Parametric sensitivity and process integration strategies. *Chem. Eng. J.* 211 (212), 122–132. doi:10.1016/j.cej.2012.09.012

Fick, A. (1855). Ueber diffusion. *Ann. Phys.* 170 (1), 59–86. doi:10.1002/andp.18551700105

Guan, G. (2017). Clean coal technologies in Japan: A review. *'Chinese J. Chem. Eng. Clean coal Technol. Jpn. A review'*, Chin. J. Chem. Eng. 25 (6), 689–697. doi:10.1016/j.cjche.2016.12.008

Hasse, D., Kulkarni, S., Sanders, E., Corson, E., and Tranier, J. P. (2013). CO2 capture by sub-ambient membrane operation. *Energy Procedia* 37, 993–1003. doi:10.1016/j.egypro.2013.05.195

He, G., Huang, S., Villalobos, L. F., Zhao, J., Mensi, M., Oveisi, E., et al. (2019). High-permeance polymer-functionalized single-layer graphene membranes that surpass the postcombustion carbon capture target. *Energy Environ. Sci.* 12 (11), 3305–3312. doi:10.1039/c9ee01238a

IEA (2021). *Global energy review: CO2 emissions in 2021*. Available at: https://www.iea.org/reports/global-energy-review-co2-emissions-in-2021-2.

IEA (2022). *International energy agency (IEA) world energy outlook 2022*. Available at: https://www.iea.org/reports/world-energy-outlook-2022.

Ji, W., Li, K., Min, Y. G., Shi, W., and Ma, X. (2021). Remarkably enhanced gas separation properties of PIM-1 at sub-ambient temperatures. *J. Membr. Sci.* 623, 119091. doi:10.1016/j.memsci.2021.119091

Ji, W., Li, K., Shi, W., Bai, L., and Ma, X. (2021). The effect of chain rigidity and microporosity on the sub-ambient temperature gas separation properties of intrinsic microporous polyimides. *J. Membr. Sci.* 635, 119439. doi:10.1016/j.memsci.2021.119439

Joglekar, M., Itta, A. K., Kumar, R., Wenz, G. B., Mayne, J., Williams, P. J., et al. (2019). Carbon molecular sieve membranes for CO2/N2 separations: Evaluating subambient temperature performance. *J. Membr. Sci.* 569, 1–6. doi:10.1016/j.memsci.2018.10.003

Kumar, R., Zhang, C., Itta, A. K., and Koros, W. J. (2019). Highly permeable carbon molecular sieve membranes for efficient CO2/N2 separation at ambient and subambient temperatures. *J. Membr. Sci.* 583, 9–15. doi:10.1016/j.memsci.2019.04.033

Lee, S., and Kim, J. K. (2020). Process-integrated design of a sub-ambient membrane process for CO2 removal from natural gas power plants. *Appl. Energy* 260, 114255. doi:10.1016/j.apenergy.2019.114255

Lee, S., Yun, S., and Kim, J. K. (2019). Development of novel sub-ambient membrane systems for energy-efficient post-combustion CO2 capture. *Appl. Energy* 238, 1060–1073. doi:10.1016/j.apenergy.2019.01.130

Li, R., Lian, S., Zhang, Z., Deng, S., and Song, C. (2022). Simulation of a novel hybrid membrane-cryogenic process for post-combustion carbon capture. *Carbon Capture Sci. Technol.* 5 (8), 100075. doi:10.1016/j.ccst.2022.100075

Li, R., Lian, S., Zhang, Z., Song, C., Han, R., and Liu, Q. (2022). Techno-economic evaluation of a novel membrane-cryogenic hybrid process for carbon capture. *Appl. Therm. Eng.* 200, 117688. doi:10.1016/j.applthermaleng.2021.117688

Liu, L., Sanders, E. S., Johnson, J. R., Karvan, O., Kulkarni, S., Hasse, D. J., et al. (2013). Influence of membrane skin morphology on CO2/N2 separation at sub-ambient temperatures. *J. Membr. Sci.* 446, 433–439. doi:10.1016/j.memsci.2013.06.001

Liu, L., Sanders, E. S., Kulkarni, S. S., Hasse, D. J., and Koros, W. J. (2014). Sub-ambient temperature flue gas carbon dioxide capture via Matrimid® hollow fiber membranes. *J. Membr. Sci.* 465, 49–55. doi:10.1016/j.memsci.2014.03.060

Mat, N. C., and Lipscomb, G. G. (2019). Global sensitivity analysis for hybrid membrane-cryogenic post combustion carbon capture process. *Int. J. Greenh. Gas Control* 81, 157–169. doi:10.1016/j.ijggc.2018.12.023

Merkel, T. C., Lin, H., Wei, X., and Baker, R. (2010). Power plant post-combustion carbon dioxide capture: An opportunity for membranes. *J. Membr. Sci.* 359 (1–2), 126–139. doi:10.1016/j.memsci.2009.10.041

Rafiq, S., Deng, L., and Hägg, M.-B. (2016). Role of facilitated transport membranes and composite membranes for efficient CO2 capture – a review. *ChemBioEng Rev.* 3, 68–85. doi:10.1002/cben.201500013

Robeson, L. M., Smith, Z. P., Freeman, B. D., and Paul, D. R. (2014). Contributions of diffusion and solubility selectivity to the upper bound analysis for glassy gas separation membranes. *J. Membr. Sci.* 453, 71–83. doi:10.1016/j.memsci.2013.10.066

Scholes, C. A., Ho, M. T., Wiley, D. E., Stevens, G. W., and Kentish, S. E. (2013). Cost competitive membrane-cryogenic post-combustion carbon capture. *Int. J. Greenh. Gas Control* 17, 341–348. doi:10.1016/j.ijggc.2013.05.017

Shafiee, A., Nomvar, M., Liu, Z., and Abbas, A. (2017). Automated process synthesis for optimal flowsheet design of a hybrid membrane cryogenic carbon capture process. *J. Clean. Prod.* 150, 309–323. doi:10.1016/j.jclepro.2017.02.151

Sharma, A., Jindal, J., Mittal, A., Kumari, K., Maken, S., and Kumar, N. (2021). *Carbon materials as CO_2 adsorbents: A review*. Springer International Publishing 19. doi:10.1007/s10311-020-01153-z

Song, C., Li, R., Fan, Z., Liu, Q., Zhang, B., and Kitamura, Y. (2020). CO2/N2 separation performance of Pebax/MIL-101 and Pebax/NH2-MIL-101 mixed matrix membranes and intensification via sub-ambient operation. *Sep. Purif. Technol.* 238, 116500. doi:10.1016/J.SEPPUR.2020.116500

Song, C., Liu, Q., Deng, S., Li, H., and Kitamura, Y. (2019). Cryogenic-based CO2 capture technologies: State-of-the-art developments and current challenges. *Renew. Sustain. Energy Rev.* 101 (2018), 265–278. doi:10.1016/j.rser.2018.11.018

Song, C., Liu, Q., Ji, N., Deng, S., Zhao, J., Li, Y., et al. (2017). Reducing the energy consumption of membrane-cryogenic hybrid CO2 capture by process optimization. *Energy* 124, 29–39. doi:10.1016/j.energy.2017.02.054

Song, C., Liu, Q., Ji, N., Deng, S., Zhao, J., Li, Y., et al. (2018). Alternative pathways for efficient CO2 capture by hybrid processes—a review. *A review'* 82 (9), 215–231. doi:10.1016/j.rser.2017.09.040

Stannett, V. T., Koros, W. J., Paul, D. R., Lonsdale, H. K., and Baker, R. W. (1979). "Recent advances in membrane science and technology," in *Chemistry* (Berlin, Heidelberg: Springer Berlin Heidelberg), 69–121. doi:10.1007/3-540-09442-3_5

Swisher, J. A., and Bhown, A. S. (2014). "Analysis and optimal design of membrane-based CO2 capture processes for coal and natural gas-derived flue gas," in *Energy procedia* (Elsevier Ltd), 225–234. doi:10.1016/j.egypro.2014.11.024

Wang, Y., Zhao, L., Otto, A., Robinius, M., and Stolten, D. (2017). A review of post-combustion CO 2 capture technologies from coal-fired power plants. *Energy Procedia* 114 (2016), 650–665. doi:10.1016/j.egypro.2017.03.1209

Weng, Y., Ji, W., Ye, C., Dong, H., Gao, Z., Li, J., et al. (2022). Simultaneously enhanced CO2 permeability and CO2/N2 selectivity at sub-ambient temperature from two novel functionalized intrinsic microporous polymers. *J. Membr. Sci.* 644, 120086. doi:10.1016/j.memsci.2021.120086

Xu, J., and Lin, W. (2017). A CO2 cryogenic capture system for flue gas of an LNG-fired power plant. *Int. J. Hydrogen Energy* 42 (29), 18674–18680. doi:10.1016/j.ijhydene.2017.04.135

Zhang, X., Singh, B., He, X., Gundersen, T., Deng, L., and Zhang, S. (2014). Post-combustion carbon capture technologies: Energetic analysis and life cycle assessment. *Int. J. Greenh. Gas Control* 27, 289–298. doi:10.1016/j.ijggc.2014.06.016